

UCSF

UC San Francisco Previously Published Works

Title

The phosphatase CD148 promotes airway hyperresponsiveness through SRC family kinases

Permalink

<https://escholarship.org/uc/item/8zc0777m>

Journal

Journal of Clinical Investigation, 123(5)

ISSN

0021-9738

Authors

Katsumoto, Tamiko R

Kudo, Makoto

Chen, Chun

et al.

Publication Date

2013-05-01

DOI

10.1172/jci66397

Peer reviewed



The phosphatase CD148 promotes airway hyperresponsiveness through SRC family kinases

Tamiko R. Katsumoto,¹ Makoto Kudo,² Chun Chen,² Aparna Sundaram,² Elliott C. Callahan,¹ Jing W. Zhu,¹ Joseph Lin,³ Connor E. Rosen,¹ Boryana N. Manz,¹ Jae W. Lee,⁴ Michael A. Matthay,^{4,5} Xiaozhu Huang,² Dean Sheppard,² and Arthur Weiss^{1,6}

¹Division of Rheumatology and Rosalind Russell Medical Research Center for Arthritis, and ²Lung Biology Center, Department of Medicine, University of California San Francisco (UCSF), San Francisco, California, USA. ³Department of Biology, Sonoma State University, Rohnert Park, California, USA. ⁴Department of Anesthesiology, UCSF, San Francisco, California, USA. ⁵Cardiovascular Research Institute, Department of Medicine, UCSF, San Francisco, California, USA. ⁶Howard Hughes Medical Institute, Chevy Chase, Maryland, USA.

Increased airway smooth muscle (ASM) contractility and the development of airway hyperresponsiveness (AHR) are cardinal features of asthma, but the signaling pathways that promote these changes are poorly understood. Tyrosine phosphorylation is tightly regulated by the opposing actions of protein tyrosine kinases and phosphatases, but little is known about whether tyrosine phosphatases influence AHR. Here, we demonstrate that genetic inactivation of receptor-like protein tyrosine phosphatase J (*Ptprj*), which encodes CD148, protected mice from the development of increased AHR in two different asthma models. Surprisingly, CD148 deficiency minimally affected the inflammatory response to allergen, but significantly altered baseline pulmonary resistance. Mice specifically lacking CD148 in smooth muscle had decreased AHR, and the frequency of calcium oscillations in CD148-deficient ASM was substantially attenuated, suggesting that signaling pathway alterations may underlie ASM contractility. Biochemical analysis of CD148-deficient ASM revealed hyperphosphorylation of the C-terminal inhibitory tyrosine of SRC family kinases (SFKs), implicating CD148 as a critical positive regulator of SFK signaling in ASM. The effect of CD148 deficiency on ASM contractility could be mimicked by treatment of both mouse trachea and human bronchi with specific SFK inhibitors. Our studies identify CD148 and the SFKs it regulates in ASM as potential targets for the treatment of AHR.

Introduction

Asthma affects 300 million persons worldwide and continues to increase in prevalence, carrying a substantial economic impact (1). Asthma is characterized by chronic airway inflammation, variable airflow obstruction, and increased sensitivity of the airways to inhaled constrictor agents, referred to as airway hyperresponsiveness (AHR). Severe asthmatics often do not respond adequately to corticosteroid therapy (2, 3), highlighting the need for novel therapeutic approaches. The development of AHR in human asthma involves the complex interplay between the immune system, the airway epithelium, and the mesenchymal cells involved in airway remodeling. The molecular basis for AHR remains incompletely characterized, however intrinsic differences in airway smooth muscle (ASM) function have been implicated (4, 5). Possible mechanisms by which ASM could contribute to AHR include modulation of excitation-contraction coupling mechanisms, interactions between locally infiltrating mast cells and ASM, hyperplasia and/or hypertrophy leading to increased ASM mass, and other alterations in biophysical properties (6–9). However, ASM and the signaling pathways regulating ASM contractility, are likely to play a paramount role.

The importance of tyrosine phosphorylation pathways in asthma is becoming increasingly appreciated (2, 10). Tyrosine phosphorylation signaling pathways are regulated not only by protein tyrosine kinases (PTKs), but also by protein tyrosine

phosphatases (PTPs), which are less well understood. CD148, also known as *Ptprj* or DEP-1, is a receptor-like protein tyrosine phosphatase (RPTP) that is comprised of an extracellular domain consisting of 8 fibronectin-type repeats, a transmembrane domain, and a cytoplasmic phosphatase domain. CD148 is highly expressed on both hematopoietic and nonhematopoietic cells, including cells of the lung (11–13). The physiologic function of CD148 outside of the hematopoietic system remains obscure, although it has been shown to be upregulated in epithelial cells grown at high density and has been implicated in regulating contact inhibition of cell growth. Recently, thrombospondin-1 (14) and syndecan-2 (15) were reported to specifically interact with the extracellular domain of CD148; however, the functional consequences of these interactions are unclear.

Both receptor tyrosine kinases and nonreceptor tyrosine kinases play critical roles in a variety of cell types in asthma, and several tyrosine kinase inhibitors have demonstrated efficacy in animal models of asthma (2, 10). SFKs, composed of 9 different nonreceptor tyrosine kinases, play critical proximal roles in many signaling pathways implicated in asthma pathogenesis, including those of antigen receptors, growth factor receptors, G protein-coupled receptors (GPCRs), and integrins (16). Individual SFKs are differentially expressed in various cell types, and details concerning the regulation of their activity remain incompletely understood. SFKs are tightly regulated by two critical tyrosine phosphorylation sites: a tyrosine in the kinase activation loop that, when trans-autophosphorylated, contributes to increased catalytic activity, and a C-terminal inhibitory tyrosine that, when phosphorylated by

Conflict of interest: The authors have declared that no conflict of interest exists.

Citation for this article: *J Clin Invest.* 2013;123(5):2037–2048. doi:10.1172/JCI66397.

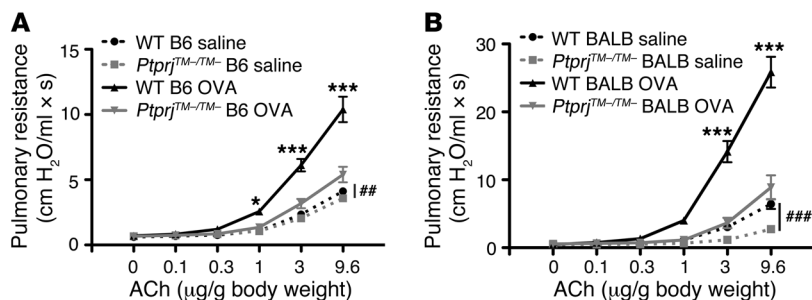


Figure 1 CD148-deficient mice are protected from AHR in the OVA mouse model of allergic airway disease and have decreased baseline pulmonary resistance. (A) Pulmonary resistance measurements in WT and CD148-deficient (*Ptprj*^{TM-/TM-}) mice following immunization and intranasal challenge with OVA or saline in C57BL/6 mice (A) or BALB/c mice (B). Data are the mean ± SEM (n = 9–13 animals per group). Statistical significance determined by 2-way ANOVA. *P < 0.05, ***P < 0.001 in the WT versus *Ptprj*^{TM-/TM-} OVA group; ##P < 0.01, ###P < 0.001 comparing the highest dose of ACh in the WT saline group with the *Ptprj*^{TM-/TM-} saline group.

the kinase CSK, leads to stabilization of an autoinhibited, closed conformation (17, 18). We have previously shown that two RPTPs, CD45 and CD148, positively regulate SFKs in B cell and macrophage immunoreceptor signaling by dephosphorylating the C-terminal inhibitory tyrosine of SFKs (19). In fibroblasts and epithelial cells, nonhematopoietic cells that lack CD45, the phosphatases RPTPα and PTP1B have been primarily implicated in dephosphorylating the C-terminal negative regulatory tyrosine of SFKs (20–22). However, the tyrosine phosphatases that regulate SFK activity in ASM remain undefined.

Here, we evaluated the impact of the phosphatase CD148 on the development of acute allergic airway disease. Based on our prior studies of CD148 in hematopoietic cells, which revealed its positive regulatory function via SFKs in various receptor systems and the complex role of hematopoietic cells in asthma pathogenesis (19), we hypothesized that CD148 deficiency would decrease SFK activity, leading to attenuation of experimental asthma. We observed striking protection from the development of AHR in mice lacking CD148 phosphatase activity, but surprisingly, this was not a consequence of CD148 activity in the hematopoietic or endothelial lineages. We identify CD148 as a critical positive regulator of SFK activity in ASM, thereby contributing to the blunted development of AHR in CD148-deficient mice. This work highlights what we believe to be a novel and important mechanism by which SFKs are regulated in ASM and suggests a therapeutic strategy for targeting asthma pathogenesis.

Results

CD148 promotes AHR but minimally affects the inflammatory response following OVA sensitization and challenge. We investigated the influence of CD148 on the development of acute allergic airway disease by using previously described *Ptprj*^{TM-/TM-} mice (19) that carry a constitutive deletion of the transmembrane domain, leading to loss of CD148 phosphatase activity. A secreted extracellular domain of CD148 was found in the serum of *Ptprj*^{TM-/TM-} mice, but CD148 was not detected on any hematopoietic cells (19) or other nonhematopoietic lung cells based on immunofluorescence staining. Additionally, heterozygous mice phenocopied WT mice, suggesting no dominant negative effect of the secreted protein.

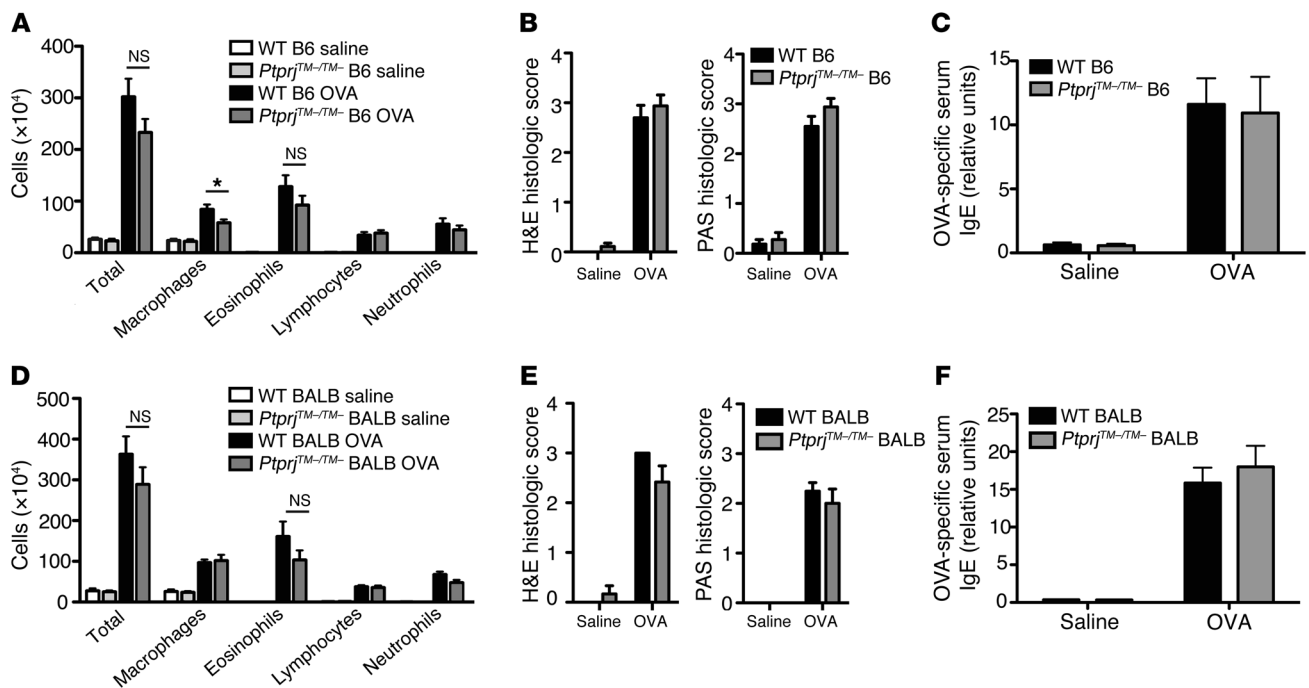
Control (WT) and CD148 phosphatase-deficient (*Ptprj*^{TM-/TM-}) mice were sensitized by 3 weekly intraperitoneal injections of OVA and alum adjuvant versus alum adjuvant only (saline controls), followed by 3 consecutive days of intranasal challenge with OVA or saline. Invasive pulmonary function testing revealed a substantial reduction in AHR in OVA-sensitized and challenged *Ptprj*^{TM-/TM-} mice compared with WT mice of the C57BL/6 background (Figure 1A). WT and *Ptprj*^{TM-/TM-} mice of the BALB/c strain, which have increased baseline AHR, are more atopic, and are known to develop increased AHR in response to allergen challenge (23), also showed similarly attenuated AHR in the *Ptprj*^{TM-/TM-} mice compared with the WT mice following allergen challenge (Figure 1B). These findings suggest that the influence of CD148 on AHR was not strain specific. Intriguingly, unsensitized *Ptprj*^{TM-/TM-} mice of both C57BL/6 and BALB/c strains demonstrated a significant attenuation

in baseline airway reactivity to acetylcholine (ACh), suggesting that intrinsic differences in ASM contractility could contribute to the observed phenotype (Figure 1, A and B).

We previously showed that CD148 deficiency influences the responses of B cells, macrophages, neutrophils, and platelets to certain receptor stimuli (19, 24, 25). Therefore, we examined whether attenuation of the immune response was primarily responsible for the reduction in AHR observed in *Ptprj*^{TM-/TM-} mice. Surprisingly, WT and *Ptprj*^{TM-/TM-} control mice and OVA-challenged mice of both the C57BL/6 and BALB/c strains exhibited no consistent differences in the accumulation of cells in the bronchoalveolar lavage (BAL). Similar numbers of macrophages, lymphocytes, eosinophils, and neutrophils were present in the lavage fluids (Figure 2, A and D). H&E staining of lung sections revealed no attenuation of inflammation in *Ptprj*^{TM-/TM-} mice (Figure 2, B and E, left panels, and Supplemental Figure 1; supplemental material available online with this article; doi:10.1172/JCI66397DS1). Airway epithelial production of mucus, a prominent feature of asthmatic airways, can be driven by the Th2 cytokine IL-13 (26). Period acid-Schiff (PAS) staining of lung sections highlights mucus staining, and no significant differences were observed between WT and *Ptprj*^{TM-/TM-} mice of either strain (Figure 2, B and E, right panels). Moreover, serum levels of OVA-specific IgE were not different between WT and *Ptprj*^{TM-/TM-} mice of both strains (Figure 2, C and F). Taken together, the findings of diminished AHR coupled with a preserved inflammatory response suggest a dissociation of the two processes.

Although the heterogeneity of human asthma is becoming increasingly appreciated (27), in many cases it is thought to reflect the consequence of Th2-dominated immune responses to allergens, with the cytokines IL-4 and IL-13 playing prominent roles (28, 29). The OVA mouse model of asthma is largely driven by Th2 cytokines (30). Following OVA sensitization and challenge, we carefully evaluated the immune response by intracellular cytokine staining of T cell subsets isolated from the lung and mediastinal lymph nodes of BALB/c mice. We observed no differences in the absolute numbers or percentages of mediastinal lymph node or lung T cell subsets secreting the cytokines IL-4 and IL-13 (Figure 3, A–E and G).

Recent studies have highlighted the complexity of the immune response underlying some subsets of asthma, with potential

**Figure 2**

CD148 deficiency does not attenuate inflammatory response following OVA allergen sensitization and challenge. (A and D) BAL cell counts of total cells, macrophages, eosinophils, lymphocytes, and neutrophils in WT and CD148-deficient (*Ptprj*^{TM-TM}) mice following immunization and intranasal challenge with OVA or saline in C57BL/6 (A) or BALB/c (D) mice. (B and E) Histologic scoring on a scale of 0 to 4 by a blinded observer of H&E staining to quantify the degree of airway inflammation (left panel) and PAS staining to quantify mucus-producing goblet cells (right panel) in WT and *Ptprj*^{TM-TM} mice. (C and F) Relative OVA-specific serum IgE levels were measured by ELISA in WT and *Ptprj*^{TM-TM} mice. Data for all panels include 9–13 animals per group. Data show the mean ± SEM. **P* < 0.05, unpaired 2-tailed Student's *t* test. NS, nonsignificant.

contributions from the Th1 and Th17 immune arms (31, 32). We therefore also examined mediastinal lymph node and lung T cell subsets producing IFN γ and IL-17 and found no significant differences in numbers or percentages of these cells between OVA-sensitized and -challenged WT and *Ptprj*^{TM-TM} BALB/c mice (Figure 3, F and H–L).

CD148-deficient mice are protected from AHR induced by house dust mite. Although the OVA-induced model of allergic airway disease is one of the most widely used, an important limitation is that OVA is not an antigen that triggers human asthma. Another caveat is that sensitization with OVA through the respiratory tract is not generally successful, thus intraperitoneal sensitization in conjunction with adjuvant is conventionally used (33). Therefore, we opted to extend our studies to the house dust mite (HDM) model, which utilizes a known human antigen and involves sensitization through the respiratory mucosa and thus may better recapitulate human asthma. We found that AHR was similarly attenuated both at baseline and following HDM antigen sensitization and challenge in *Ptprj*^{TM-TM} mice (Figure 4A). A slight, but statistically significant, decrease in BAL lymphocytes and macrophages and PAS histologic staining was observed in *Ptprj*^{TM-TM} mice compared with control mice, but other inflammatory parameters were not significantly affected (Figure 4, B–D). Collectively, these studies suggest the possibility that the protection afforded to mice by the loss of the CD148 phosphatase in 2 experimental models of asthma and in 2 strains of mice might not reflect a substantial effect of CD148 on the immune responses mediated by hematopoietic cells.

Hematopoietic and endothelial lineage deletion of CD148 does not affect AHR. Since CD148 is expressed on hematopoietic as well as on nonhematopoietic cells, and the contribution of the Th2 immune response in asthma is very well documented (34), we wanted to further verify that the protection afforded by CD148 deficiency was indeed independent of its function in hematopoietic lineage cells. Using mice harboring a floxed allele of CD148 (which also eliminates the membrane-encoding exon) that allows for the lineage-specific inactivation, CD148 function was eliminated from hematopoietic and endothelial cells using a *Vav1-Cre* transgene (*Ptprj*^{TM-fl/TM};*Vav-Cre*). B cells (Figure 5A) and monocytes (data not shown) from *Ptprj*^{TM-fl/TM};*Vav-Cre* mice verified CD148 deletion efficiency comparable to *Ptprj*^{TM-TM} constitutively deleted cells. When these mice were challenged with OVA, there was no statistically significant difference in the development of AHR when CD148 was deleted from hematopoietic and endothelial cells (*Ptprj*^{TM-fl/TM};*Vav-Cre* mice) as compared with control mice (Figure 5B). Additionally, baseline pulmonary airway resistance was unaffected by deletion of CD148 from these lineages. The inflammatory response revealed an increase in total BAL cell counts in *Ptprj*^{TM-fl/TM};*Vav-Cre* mice, which was largely driven by an increase in neutrophils, but other cell types were comparable to control groups (Figure 5C). Likewise, histologic scores and serum IgE did not differ in the *Vav-Cre*-targeted mice compared with the responses of control mice (Figure 5, D and E). Collectively, these results support the notion that CD148 protection from induced AHR is independent of its expression in hematopoietic lineage cells.

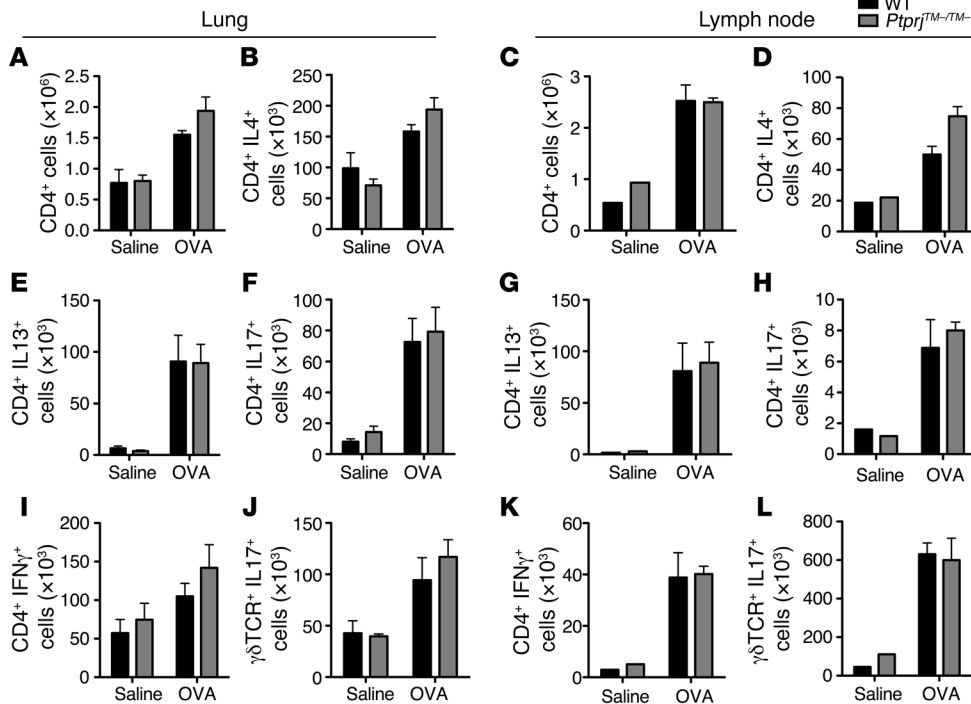


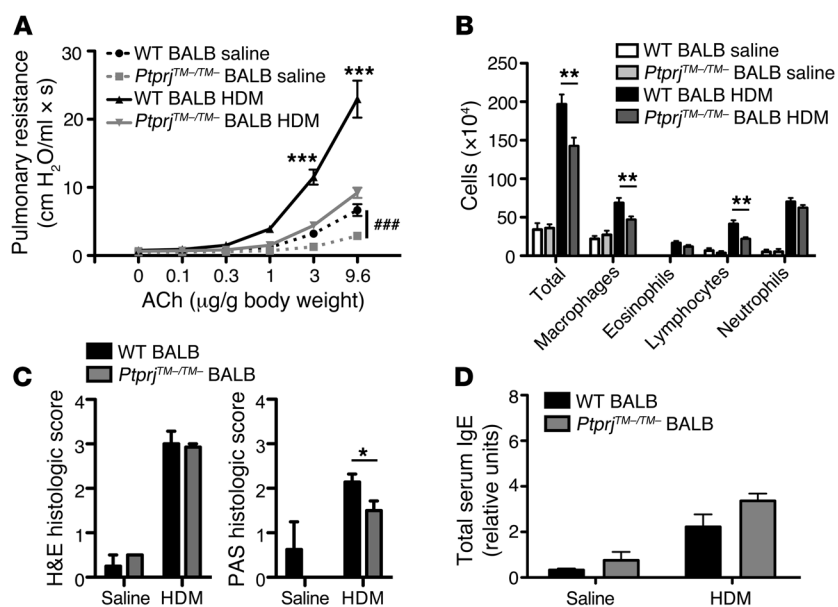
Figure 3 CD148 does not regulate T cell immune responses to allergen. BALB/c mice were immunized and sensitized with OVA, and cells from the lungs and mediastinal lymph nodes were stimulated with PMA and ionomycin and analyzed using intracellular cytokine staining. Total CD4 counts were similar in lung (A) and mediastinal lymph node (C). Absolute numbers of CD4⁺ IL4⁺ (B and D), CD4⁺ IL13⁺ (E and G), CD4⁺ IL17⁺ (F and H), CD4⁺ IFNγ⁺ (I and K), and γδTCR⁺ IL17⁺ (J and L) cells in both lung and lymph node were not statistically significantly different by unpaired 2-tailed Student's *t* test. Data are the mean ± SEM for at least 5 mice per group.

Partial deletion of CD148 from smooth muscle leads to attenuation of AHR. Since CD148 is expressed in smooth muscle, we wondered whether CD148 phosphatase function in ASM could be contributing to AHR. We therefore generated mice specifically lacking CD148 in smooth muscle by crossing our *Ptprij*^{TM-β/TM-β} mice with mice expressing the reverse tetracycline transactivator under the control of the α-smooth muscle actin promoter (α-SMA-rTTA) and (tetO)₇-Cre (35). The tissue specificity of deletion in smooth muscle has been previously confirmed (36). Mice carrying all 4 alleles will be referred to as *Ptprij*^{TM-β/TM-β};SMA-rTTA Cre. Immunofluorescence demonstrated a substantial reduction of CD148 expression in tracheal smooth muscle (Figure 6A), however, CD148 deletion appeared to be less complete in bronchial ASM (Supplemental Figure 2). There were no apparent differences in the volume of ASM tissue, as determined by using α-SMA staining, between *Ptprij*^{TM-β/TM-β};SMA Cre mice and *Ptprij*^{TM-β/TM-β} Cre mice (data not shown). A caveat of this strategy is that deletion of the floxed CD148 allele is not specific to ASM, as it would also occur in vascular smooth muscle.

Mice with the deletion of CD148 in smooth muscle (*Ptprij*^{TM-β/TM-β};SMA-rTTA Cre) demonstrated diminished AHR compared with *Ptprij*^{TM-β/TM-β} Cre mice, however the magnitude of diminution was less profound than in constitutively deleted mice (Figure 6B). The inflammatory response was comparable between *Ptprij*^{TM-β/TM-β};SMA-rTTA Cre and control *Ptprij*^{TM-β/TM-β} Cre mice, as measured by BAL cell accumulation (Figure 6C), mucus production (Figure 6D), and OVA-specific IgE production (Figure 6E). The less robust protection from AHR could be a consequence of incomplete deletion of CD148 from bronchial ASM, as well as the possibility that CD148 acts on other cell types, such as airway epithelium that could be mediating AHR. Nonetheless, the statistically significant reduction in AHR in *Ptprij*^{TM-β/TM-β};SMA Cre mice illustrates an impact of CD148 on signaling pathways in ASM, cells that play a critical role in bronchoconstriction.

Absence of CD148 phosphatase activity impairs tracheal contractility and SFK activation. ASM contraction occurs via GPCR activation, such as through G_q-coupled muscarinic, histamine, endothelin, thromboxane, and cysteinyl leukotriene receptors, and G_i-coupled 5-HT and adenosine receptors (37). Stimulation of the G_q receptor in ASM leads to activation of phospholipase C beta (PLCβ), which hydrolyzes phosphoinositol 4,5-bisphosphonate (PIP₂) into 1,2-diaclyglycerol (DAG) and inositol 1,4,5-triphosphate (IP₃). Increased IP₃ and DAG levels stimulate an increase in intracellular Ca²⁺ through release from internal stores and influx from membrane-bound channels and activation of PKC. The rise in intracellular calcium promotes calcium binding to calmodulin, which complexes with and activates myosin light chain kinase (MLCK). MLCK phosphorylates regulatory myosin light chains (MLCs) and enables actin to activate the myosin ATPase activity required for cross-bridge cycling and contraction (38).

We hypothesized that an intrinsic difference in ASM contractility in *Ptprij*^{TM-β/TM-β} mice accounted for the attenuated AHR observed. We measured the contractility of tracheal rings from *Ptprij*^{TM-β/TM-β} and control mice following methacholine (MCh) treatment. Diminished contractility was observed following MCh stimulation of tracheal rings harvested from *Ptprij*^{TM-β/TM-β} mice (Figure 7A). We speculated that positive regulation of SFKs in ASM by CD148 accounted for the diminished contractility of *Ptprij*^{TM-β/TM-β} tracheal rings. We detected marked hyperphosphorylation of the C-terminal negative regulatory tyrosine Y527 of SRC in unstimulated CD148-deficient smooth muscle (Figure 7B), a predominant cellular component in posterior tracheal strips. This hyperphosphorylation of Y527 was highly statistically significant by densitometric analysis (Figure 7C), and is similar to what we have previously seen in B cells and macrophages deficient in both CD148 and CD45 (19), and in CD148-deficient platelets, which lack CD45 (25). The hyperphosphorylation of this negative reg-

**Figure 4**

CD148-deficient mice are protected from HDM-induced AHR with minimal attenuation of inflammatory response to allergen. (A) Pulmonary resistance measurements in WT and *Ptprj*^{TM-/TM-} BALB/c mice following immunization and intranasal challenge with HDM. ****P* < 0.001 for the WT HDM versus the *Ptprj*^{TM-/TM-} HDM group; ###*P* < 0.001 comparing the highest dose of ACh in the WT saline group with the *Ptprj*^{TM-/TM-} saline group by 2-way ANOVA. (B) BAL cell counts of total cells, macrophages, eosinophils, lymphocytes, and neutrophils in WT and *Ptprj*^{TM-/TM-} mice. (C) Histologic scoring on a scale of 0 to 4 by a blinded observer of H&E staining to quantify degree of airway inflammation (left panel) and PAS staining to quantify mucus-producing goblet cells (right panel) in WT and *Ptprj*^{TM-/TM-} mice. (D) Total serum IgE levels (relative units) measured by ELISA in WT and *Ptprj*^{TM-/TM-} mice in the HDM model. Data for all panels include at least 10 animals per group. Data show the mean ± SEM. (B–D) **P* < 0.05, ***P* < 0.01, unpaired 2-tailed Student's *t* test.

ulatory tyrosine strongly suggests that it serves as a substrate for the CD148 phosphatase, though it does not exclude the existence of other CD148 substrates in ASM. Stimulation of agarose-embedded lung slices with MCh induces circumferential calcium oscillations along the ASM, the frequency of which determines airway contractility (39). We observed a striking 2-fold decrease in calcium oscillation frequency in MCh-stimulated lung slices from *Ptprj*^{TM-/TM-} mice compared with WT mice (Figure 7, D and E, and Supplemental Videos 1 and 2), further substantiating the positive regulatory effect of CD148 on ASM contractility.

Pharmacologic inhibition of SFKs attenuates mouse tracheal contractility and human bronchial contractility. We wondered whether treatment with an SFK inhibitor might recapitulate the genetic loss of CD148 phosphatase activity. SU6656 is an SFK-specific inhibitor targeting SRC, YES, FYN, and LYN (40), the primary SFKs found in ASM (41). Mouse tracheal rings pretreated with SU6656 had significantly diminished contractility following stimulation with MCh (Figure 8A) compared with vehicle treatment. To further substantiate that this inhibitory effect was a consequence of SFK inhibition, we used a chemically distinct and highly specific SFK inhibitor, AZD0530, which targets multiple SFK members with high potency. Treatment of WT tracheal rings with AZD0530 led to a significant decrease in tracheal contractility (Figure 8B). *Ptprj*^{TM-/TM-} tracheal rings exhibited diminished baseline contractility, as previously observed, but importantly, AZD0530 treatment of *Ptprj*^{TM-/TM-} tracheal rings did not further impair tracheal contractility, strongly arguing that the genetic loss of *Ptprj* and the inhibition of SFK were in a similar pathway (Figure 8C). Human bronchial rings pretreated with SU6656 similarly demonstrated diminished contractile force in response to MCh (Figure 8D). This observation supports the contribution of SFKs to human ASM contractility and suggests relevance to AHR in human asthma.

Discussion

Dysregulated ASM function underlies the pathogenesis of asthma and AHR (6, 42). The contraction and relaxation of ASM is primarily mediated through various GPCRs, the aberrant regulation

of which can lead to AHR (37, 43, 44). Cytokines, growth factors, integrins, and other mediators further modulate ASM function. The control of ASM contractility by tyrosine phosphatases has not been characterized. Our work provides evidence that the RPTP CD148 is a critical positive regulator of SFKs in ASM. We observed marked attenuation of AHR in mice lacking CD148 that is not primarily attributable to a dampened immune response. In addition, we report that CD148-deficient mice manifest diminished baseline pulmonary resistance in the absence of allergen sensitization and challenge, implicating decreased intrinsic ASM contractility. We provide compelling genetic, functional, and biochemical evidence that CD148 positively regulates ASM contractility via SFKs. Attenuation of AHR when CD148 is genetically deleted from smooth muscle corroborates its positive role in smooth muscle contractility, but does not exclude the possibility that other cell types, such as airway epithelium, may also be contributing to the attenuation. We show that CD148 deficiency impairs SFK activation, leading to decreased murine tracheal contractility that is recapitulated by chemical inhibition of SFKs in both murine trachea and human bronchi. Our data suggest that inhibition of CD148 phosphatase activity or specific inhibition of SFKs may be attractive therapeutic strategies for the treatment of AHR.

Surprisingly little is understood about the physiologic functions of the RPTP CD148. Most studies have been based on overexpression in cell lines or knockdown approaches, which may not accurately reflect in vivo biology. Overexpression may lead to loss of phosphatase substrate specificity, and incomplete knockdown may result in variable effects, given the complex positive and negative regulatory properties of phosphatases (45). Here, we have used a mouse carrying a targeted deletion of the CD148 transmembrane domain such that phosphatase activity was abrogated. We have previously shown that CD148, in conjunction with another RPTP, CD45, positively regulates SFKs in B cell and macrophage immunoreceptor signaling by dephosphorylating the C-terminal inhibitory tyrosine of SFKs (19). In ASM, which does not express CD45, we have discovered that the CD148 phosphatase plays a prominent role in the positive regulation of SFKs. We speculate

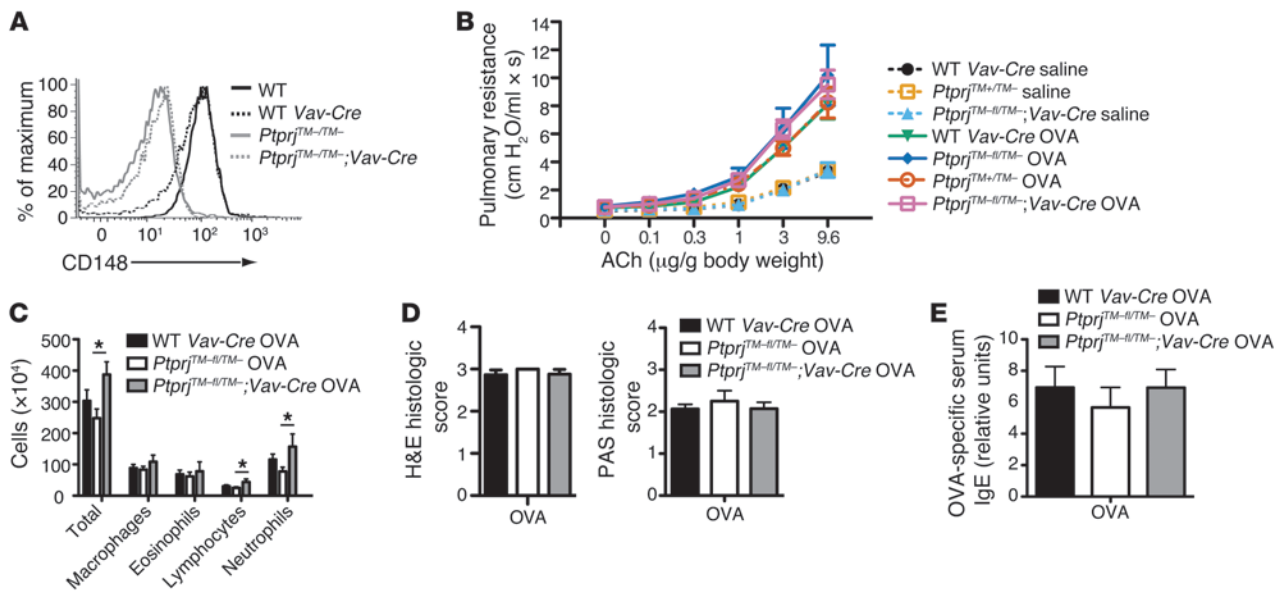


Figure 5 Deletion of CD148 on hematopoietic and endothelial cells does not attenuate AHR. **(A)** Flow cytometry plot showing deletion efficiency of CD148 gated on B220⁺ B cells of WT, WT Vav-Cre, Ptprij^{TM-/-}, and Ptprij^{TM-/-};Vav-Cre mice. Mice of the indicated genotypes were immunized and intranasally challenged with OVA or saline **(B–E)**. **(B)** Pulmonary resistance measurements after intravenous administration of increasing doses of ACh in control (WT), Ptprij^{TM+/-}, Ptprij^{TM-/-}, and Ptprij^{TM-/-};Vav-Cre mice of the C57BL/6 strain. **(C)** BAL cell counts of total cells, macrophages, eosinophils, lymphocytes, and neutrophils of WT Vav-Cre, Ptprij^{TM+/-}, and Ptprij^{TM-/-};Vav-Cre mice. **(D)** Histologic scoring by a blinded observer of H&E staining (left panel) and PAS staining of lung sections (right panel) in WT Vav-Cre, Ptprij^{TM+/-}, and Ptprij^{TM-/-};Vav-Cre mice. **(E)** Relative OVA-specific serum IgE levels measured by ELISA in WT Vav-Cre, Ptprij^{TM+/-}, and Ptprij^{TM-/-};Vav-Cre mice. Data for all panels show the means ± SEM, with 8 to 15 animals per group. *P < 0.05, 2-tailed Student's *t* test.

that the C-terminal tyrosine of SFKs may serve as the direct substrate for CD148, given that it was found to be hyperphosphorylated in CD148 phosphatase-deficient ASM tissue, though this finding does not exclude the possible existence of other CD148 substrates. Of the predominant SFKs expressed in human ASM (SRC, YES, FYN, and LYN) (41), it is unclear which of these individual SFK members most prominently contributes to the generation of AHR. Future investigation will be needed to define which SFKs are specifically targeted by CD148 in ASM. For instance, our group has recently shown that in neutrophils, CD45 and CD148 play contrasting roles in chemoattractant G protein-coupled receptor signaling, which is in part mediated by the ability of CD45 and CD148 to preferentially regulate different SFK members. Therefore, CD148 may dephosphorylate the C-terminal inhibitory tyrosine residue of specific SFKs that are critical positive regulators of ASM contractility.

Networks of cytokines, growth factors, chemokines, and neurotransmitters work in concert, exerting effects on several different cell types implicated in asthma pathogenesis (46). Given this complexity, targeting one specific mediator may have limited benefit. Various receptor and nonreceptor tyrosine kinase pathways, in both hematopoietic and structural cells, contribute to asthma pathogenesis. SRC family kinases are enzymes that proximally regulate several pathways relevant to asthma, including antigen receptors, receptor tyrosine kinases, cytokine receptors, GPCRs, and integrins (16, 47). Classical GPCRs, which are directly implicated in ASM contractile responses, activate serine/threonine kinases or ion channels regulated by second messengers leading to rapid short-term responses. Mounting evidence also implicates GPCR signaling

in the control of cell growth, proliferation, and differentiation by activating tyrosine phosphorylation cascades, including SFKs (48). SFKs can integrate the crosstalk between GPCR and RTK signaling pathways, and many mechanisms have been implicated, including the direct association of GPCRs with SFKs or other receptor-associated proteins, as well as the transactivation of RTKs and focal adhesion complexes by GPCR stimulation (16, 47, 48).

The mechanisms by which SFKs are regulated in ASM, and in particular the phosphatases that control their activation status, remain obscure (48–50). Much of our knowledge is based on the use of chemical SFK inhibitors, which not only lack selectivity for specific SFK members, but also target other kinases. Our understanding of SFKs is further complicated by the existence of multiple SFK members that may have contrasting functions as well as differing patterns of expression in various tissues. One example is the SFK LYN, which is known to play both positive and negative regulatory roles (51). Mice genetically deficient for LYN demonstrated an enhanced Th2 response and more severe asthma, likely related to the negative regulatory effects of LYN in the hematopoietic lineage (52). Therefore, in considering SFK inhibition as a potential asthma therapy, an optimal SFK inhibitor should not target LYN or the negative regulatory kinase CSK. Selective inhibitors of SFKs have been developed. As an example, the SFK inhibitor SU6656 shows selectivity for SRC, YES, FYN, and LYN, but minimally inhibits LCK, an SFK primarily expressed in T cells, or for the kinase CSK (40). Therefore, a chemical inhibitor that targets specific SFK members may be possible and preferred for therapeutic intervention.

Few studies have directly interrogated the role of SFKs in ASM, but to date none have used for in vivo genetic approaches. The

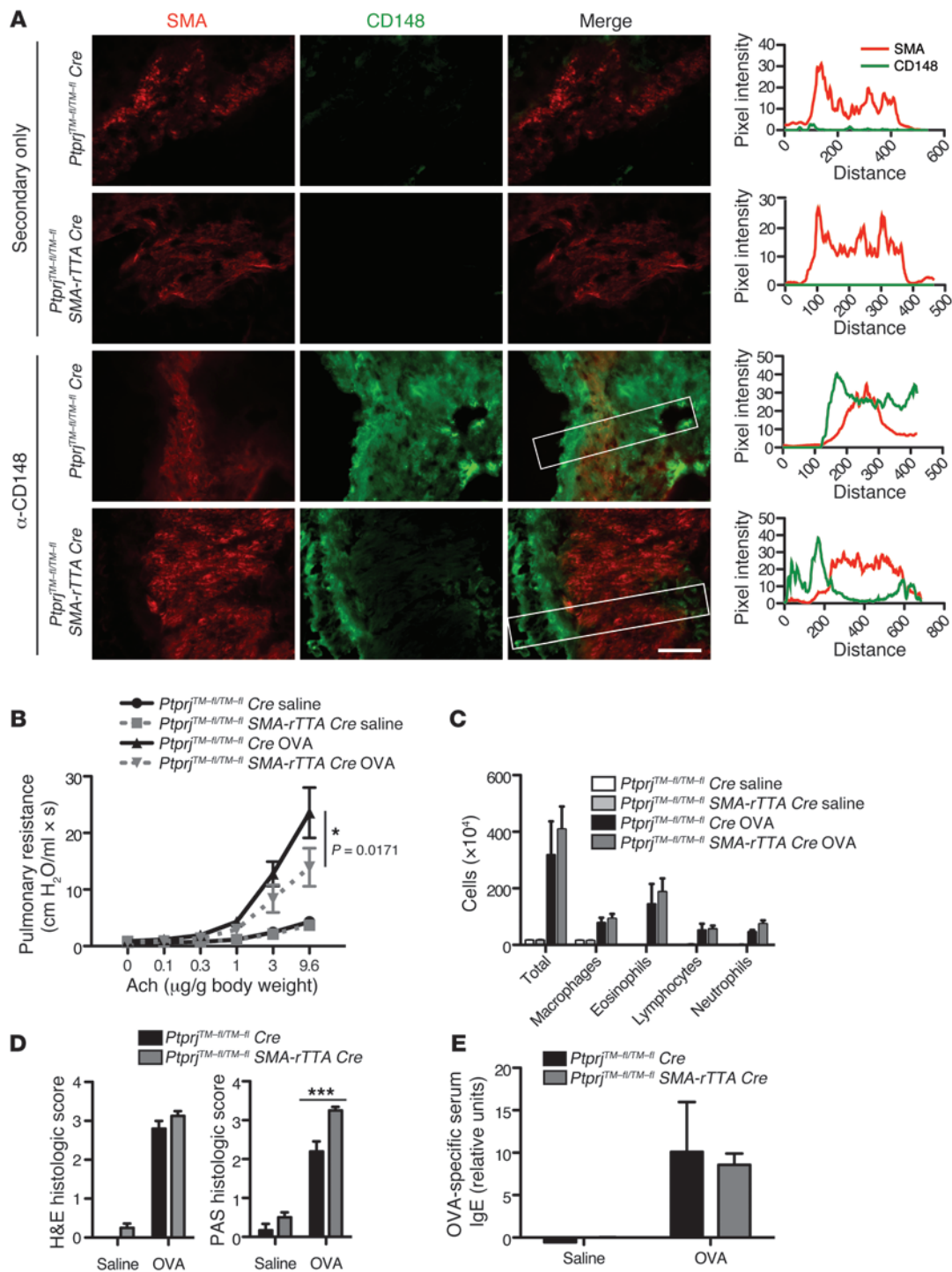


Figure 6

Partial protection from AHR in mice with deletion of CD148 from smooth muscle cells. (A) Immunofluorescence staining of mouse tracheal smooth muscle with primary hamster antibody to CD148, secondary goat anti-hamster Alexa 488 (green), and α -SMA (SMA, red) as indicated. Right column shows quantitative ImageJ analysis of line scans (areas indicated by white boxes). Mice of the indicated genotypes were immunized and intranasally challenged with OVA or saline (B–E). (B) Pulmonary resistance measurements after intravenous administration of increasing doses of ACh in *Ptprj*^{TM-*fl*/TM-*fl*};TetO-Cre and *Ptprj*^{TM-*fl*/TM-*fl*};SMA-rTTA;TetO-Cre mice of the C57BL/6 strain. **P* < 0.05 for *Ptprj*^{TM-*fl*/TM-*fl*};TetO-Cre versus *Ptprj*^{TM-*fl*/TM-*fl*};SMA-rTTA;TetO-Cre at the highest dose of ACh, 2-way ANOVA. (C) BAL cell counts of total cells, macrophages, eosinophils, lymphocytes, and neutrophils of *Ptprj*^{TM-*fl*/TM-*fl*};TetO-Cre and *Ptprj*^{TM-*fl*/TM-*fl*};SMA-rTTA;TetO-Cre mice. (D) Histologic scoring by a blinded observer of H&E-stained sections for degree of inflammation around airways (left panel) and PAS staining for PAS-positive mucus-producing goblet cells (right panel) in WT, *Ptprj*^{TM-*fl*/TM-*fl*};TetO-Cre and *Ptprj*^{TM-*fl*/TM-*fl*};SMA-rTTA;TetO-Cre mice. (E) Relative OVA-specific serum IgE levels measured by ELISA in *Ptprj*^{TM-*fl*/TM-*fl*};TetO-Cre and *Ptprj*^{TM-*fl*/TM-*fl*};SMA-rTTA;TetO-Cre mice. Data for all panels show the mean \pm SEM with 8 to 15 animals per group. Scale bar: 50 μ m (A). ****P* < 0.001, unpaired 2-tailed Student's *t* test (D).

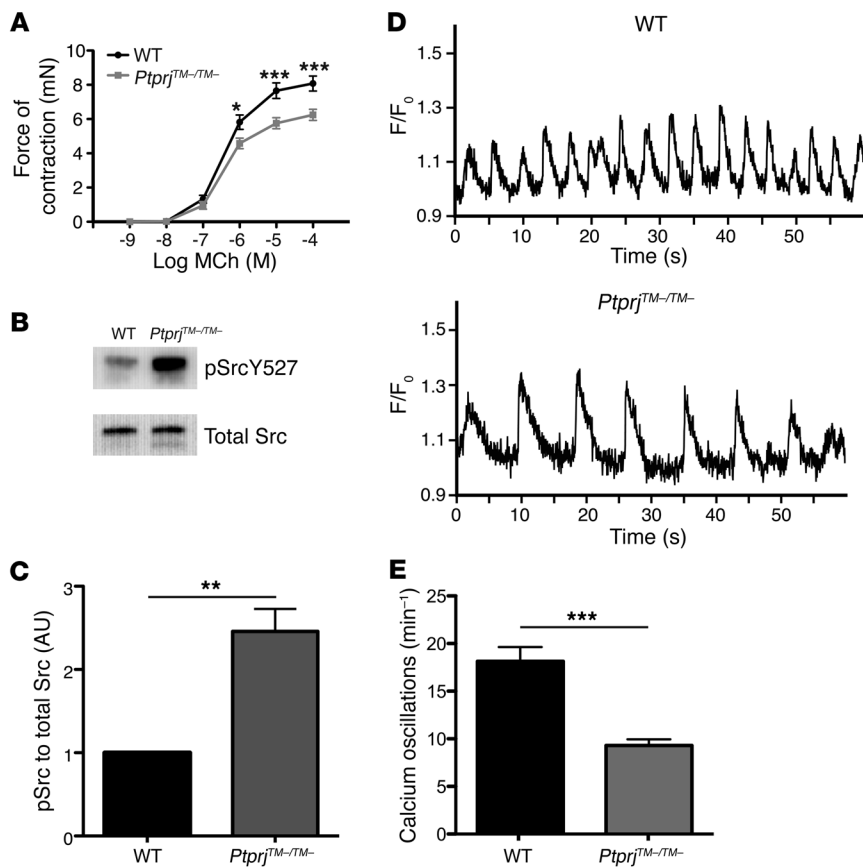


Figure 7

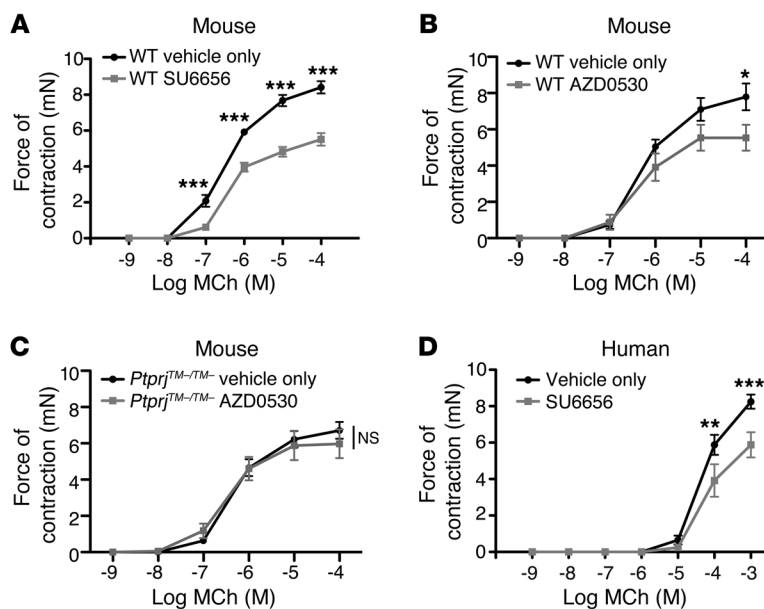
CD148-deficient tracheas show diminished contractility, decreased calcium oscillation frequency, and dysregulated SFK signaling in ASM. Mouse tracheal rings were isolated and stimulated with MCh (A), and contractile force measurements were made with a force transducer. Data are the mean ± SEM with at least 6 tracheal rings per group. **P* < 0.05, ****P* < 0.001, 2-way ANOVA. (B) Tracheal smooth muscle samples directly isolated from mice were lysed, ultracentrifuged, separated by SDS-PAGE, and transferred to a membrane. Membranes were probed with antibodies against phosphorylated SRC Y527 (inhibitory tyrosine) and total SRC as a loading control. Data shown in this figure are representative of 4 independent experiments. (C) Densitometry quantification of Western blots showing relative intensity of pSRC Y527 compared with total SRC. ***P* < 0.01, unpaired 2-tailed Student's *t* test. (D) Representative calcium oscillations induced by 50 μM MCh in lung slices from BALB/c WT control (upper panel) and *Ptprij^{TM-/TM-}* (lower panel) mice. Final fluorescence values are expressed as ratios (F/F₀), normalized to the fluorescence immediately prior to the addition of an agonist (F₀). (E) Average frequency of calcium oscillations, comparing WT control with *Ptprij^{TM-/TM-}* mice. Data include 6 animals per group. Data show the mean ± SD. ****P* < 0.001, unpaired 2-tailed Student's *t* test.

SFK inhibitor PP1, which is not highly selective, reduced the migration of human ASM cells and diminished the contractility of rat tracheal smooth muscle (50, 53, 54). SRC has been implicated in ASM proliferation and migration in response to various GPCR and receptor tyrosine kinase agonists (55). Interestingly, angiotensin II-augmented contractility of the rat left main bronchus following carbachol stimulation was attenuated by pretreatment with the SFK inhibitor SU6656 (56). However, in contrast to our studies, no inhibition of baseline rat bronchial contractility was seen with SU6656 pretreatment, which we observed in both mouse tracheal and human bronchial contractility. Perhaps species differences or contrasting technical approaches may underlie this discrepancy. In rat pulmonary artery vascular smooth muscle, the selective SRC family kinase inhibitors SU6656 and PP2 inhibited PGF_{2α}-induced contraction and MLC phosphorylation, implicating a positive regulatory role for SFKs in GPCR-mediated vascular smooth muscle contraction (57). We found that CD148-deficient ASM demonstrated more inhibition of SFKs (hyperphosphorylation of the C-terminal inhibitory tyrosine of SRC Y527) than WT ASM, and diminished the frequency of calcium oscillations and contraction following stimulation with muscarinic agonists, underscoring a critical and perhaps proximal role for SFKs in the activation of this contractile pathway.

ASM calcium oscillations induced by muscarinic agonists are, in part, mediated by the binding of IP₃ to the IP₃ receptor (IP₃R), calcium release from the sarcoplasmic reticulum, and complex feedback circuitry (58). We provide strong evidence that the tyrosine phosphatase CD148 modulates this pathway, although the exact mechanisms at play remain unclear. CD148 may regulate GPCR

sensitization and/or desensitization through its effects on SFKs or other substrates. Another possibility could be modification of the IP₃ receptor itself via tyrosine phosphorylation, which was shown to occur in T cells by the SFK FYN (59). Oscillation frequency is also regulated by sarcoplasmic reticulum (SR) calcium content and is dependent on the refilling of SR stores via the sarcoplasmic/endoplasmic reticulum Ca²⁺ ATPase (SERCA) pumps and via calcium influx from extracellular sources. How CD148 influences these pathways remains an important area for future investigation, and, notably, the intersection of tyrosine phosphorylation pathways with pathways regulating calcium oscillations has not been well characterized. One exciting possibility is that the positive regulatory role of CD148 on SFKs may regulate transient receptor potential (TRP) channels, which are phosphorylated by SRC (60–62), and by this mechanism, CD148 may regulate calcium oscillation frequency. This is certainly a high priority for future investigation.

SFKs are proximally involved in modulating several receptor tyrosine kinase (RTK) growth factors that have been implicated in asthma pathogenesis such as EGFR, VEGFR, PDGFR, and c-KIT (2, 10). There exists evidence for both negative and positive regulation of RTK signaling by CD148 (63–65), suggesting that the role of CD148 may be context dependent. Consistent with our studies, other groups have reported that CD148 is a positive regulator of SFKs via dephosphorylation of the C-terminal inhibitory tyrosine of SFKs in thyroid carcinoma (66) as well as in endothelial cells (65). Although we did not directly evaluate the effect of the CD148 phosphatase on RTK signaling pathways in ASM, it is conceivable that CD148 could be playing an important regulatory role through its influence on SFKs.

**Figure 8**

Inhibition of SRC family kinases recapitulates CD148 deficiency and leads to impaired contractility of mouse tracheal rings and human bronchial rings. Mouse tracheal rings were isolated and pretreated with the specific SRC family kinase inhibitor SU6656 at 10 μ M for 12 hours prior to stimulation with MCh (A), and contractile force measurements were made with a force transducer. Mouse tracheal rings from WT (B) or *Ptprj*^{TM-TM-} (C) mice were isolated and pretreated with the specific SRC family kinase inhibitor AZD0530 at 5 μ M for 12 hours prior to stimulation with MCh. * $P < 0.05$, 2-way ANOVA. (D) Human bronchial rings isolated from an explanted human lung were pretreated with SU6656 at 10 μ M or vehicle for 1 hour prior to stimulation with MCh and contractile force was measured. Data are the means \pm SEM for 5 to 6 mouse tracheal rings (A–C) and 6 human bronchial rings (D) per condition. ** $P < 0.01$, *** $P < 0.001$, 2-way ANOVA.

SFKs are critical regulators of integrins, which transmit signals via focal adhesion kinase (FAK) and focal adhesion signaling complexes that affect the actin cytoskeleton, an important determinant of ASM contractility (67). CD148 has been shown to play a positive regulatory role in platelet integrin function via SFK regulation (25). Future studies will more closely examine the role of CD148 in ASM integrin function and activation of focal adhesion complexes, other mechanisms by which CD148 could impact ASM contractility. CD148 function in ASM contractility could potentially be regulated by binding its recently identified ligands, thrombospondin-1 (TSP1) and syndecan-2, proteins that modulate interactions with extracellular matrix components (14, 15). For example, TSP1 stimulates vascular smooth muscle cell migration through FAK, so it is plausible that TSP1 interactions with CD148 could regulate ASM contractility (68).

Although the exact mechanisms by which the CD148 phosphatase and SFKs are involved in AHR remain incompletely defined, our data strongly suggest that the CD148 phosphatase is a critical positive regulator of SFK activity in ASM. These data present exciting new strategies for asthma treatment, focusing on the inhibition of ASM contractility. We propose two potential therapeutic approaches for asthma, directed at ASM: (a) inhibition of CD148 phosphatase activity through targeting the CD148 extracellular domain and/or modulating interactions with its ligands; or (b) inhibition of SFKs. Strategically designed inhaled inhibitors of the CD148 phosphatase or of specific SFKs could directly impact ASM function and AHR with minimal systemic side effects.

Methods

Mice

Mice constitutively lacking the CD148 (*Ptprj*) transmembrane domain were generated as previously described (19) on C57BL/6 and BALB/c backgrounds, both of which were backcrossed at least 10 generations. Mice with a floxed CD148 transmembrane allele were generated by inserting loxP recombination sites flanking the CD148 transmembrane

exon 18. Conditional deletion of the CD148 floxed allele on hematopoietic and endothelial cells was achieved by crossing *Ptprj*^{TM- β TM-} mice with *Vav1-Cre* (*Vav-Cre*) transgenic mice, as previously described (69). α -SMA-*rTTA* mice were provided by M. Shipley (Washington University School of Medicine, St. Louis, Missouri, USA) and have been previously described (36). The (*TetO*)-*Cre* mouse line has been previously described (35). All animals used were between 8 and 16 weeks of age. Sex-matched littermate controls were used in all experiments for AHR studies. For tracheal ring contractility measurements and lung slice calcium oscillation studies, BALB/c strains were used.

Antibodies and reagents

Anti-murine CD148 mAb (8A-1) was generated as previously described (12). Secondary goat anti-hamster FITC antibody was from Invitrogen, and secondary goat anti-hamster Alexa 488 antibody was from Molecular Probes (Invitrogen). The following antibodies were from BD Biosciences – Pharmingen: anti-CD4 (clone GK1.5); anti-CD8 α (clone 53-6.7); anti- $\gamma\delta$ TCR (clone GL-3); anti-CD45R/B220 (clone RA3-6B2); and anti-IFN γ . The following antibodies were from eBioscience: anti-IL-13 (clone eBio 13A) and anti-IL-17A (clone eBio 17B7). Antibodies against phospho-SRC (Tyr527) and total SRC were from Cell Signaling Technology.

Murine models of allergic airway disease

OVA-alum model. Six- to 8-week-old sex-matched *Ptprj*^{TM-TM-} and littermate control mice were sensitized on days 0, 7, and 14 by intraperitoneal injection of 50 μ g OVA (Sigma-Aldrich) emulsified in 1 mg of aluminum potassium sulfate. Control animals received an equal volume of emulsified saline/aluminum potassium sulfate. Subsequently, mice were anesthetized with isoflurane and intranasally challenged on 3 consecutive days (days 21, 22, and 23) by aspiration of 100 μ g OVA dissolved in 40 μ l saline.

HDM model. Mice were anesthetized with isoflurane prior to intranasal aspiration of 40 μ l of dust mite fecal pellet preparation (2.5 mg/ml; Greer Laboratories) or saline on days 0, 21, 22, and 23.

Twenty-four hours after the last challenge, mice were anesthetized with ketamine (100 mg/kg of body weight), xylazine (10 mg/kg), and acepromazine (3 mg/kg). Pulmonary resistance was determined using invasive cannulation of the trachea as previously described (36).



Assessment of pulmonary inflammation and mucus production

Lungs were subjected to 5 consecutive lavages with 0.8 ml of PBS. After lysing red blood cells, the total cells were counted with a hemocytometer. Cytospin preparations were stained with a HEMA 3 stain set (Fisher Scientific), and cell differential percentages were determined based on light microscopic evaluation of greater than 300 cells per slide. Lavaged lungs were inflated with 10% buffered formalin to 25 cm H₂O of pressure. Multiple paraffin-embedded 5- μ m sections of the entire mouse lung were prepared and stained with H&E and PAS to evaluate mucus production.

Assessment of serum IgE levels

Sera were obtained from blood collected by cardiac puncture from antigen- or vehicle-treated mice after airway responsiveness measurements. Serum IgE levels were measured by enzyme-linked immunosorbent assay using microplates coated with OVA (OVA-specific IgE) or anti-mouse IgE (total IgE, R35-72; BD Biosciences – Pharmingen). Diluted serum samples were added to each well, and the bound IgE was detected with biotinylated anti-mouse IgE (R35-118; BD Biosciences – Pharmingen). Color development was achieved using streptavidin-conjugated HRP (BD Biosciences – Pharmingen) followed by the addition of HRP substrate (TMB; BD Biosciences – Pharmingen).

Intracellular cytokine staining

Mediastinal lymph nodes and lung were isolated, minced, and dispersed through 70- μ m nylon filters and washed. After red blood cell lysis, cells were incubated for 4 hours at 37°C in RPMI containing 50 ng/ml PMA (Sigma-Aldrich), 1 μ M ionomycin (Sigma-Aldrich), and 10 μ g/ml brefeldin A (Epicentre). Cells were then resuspended in PBS/2% FCS and stained with the indicated antibodies for cell surface markers and intracellular cytokines. DAPI exclusion identified live cells, and samples were analyzed on a FACSCalibur flow cytometer (BD Biosciences), Gallios (Beckman Coulter), or LSR II (BD Biosciences). Data were analyzed with FlowJo software (TreeStar).

Tracheal and bronchial ring contractility assays

Tracheal ring contractility assays were performed as previously described (70). In some experiments, tracheal rings were preincubated with SU6656 (Sigma-Aldrich) at 10 μ M or AZD0530 at 5 μ M (Selleck Chemicals) in a 37°C incubator with 5% CO₂.

Human bronchi with a diameter between 5 and 8 mm were dissected free of lung connective tissue and cut into 4-mm-thick rings. The rings were then stored overnight at 37°C in DMEM medium. Bronchi were preincubated with DMSO alone or with 10 μ M SU6656 (Sigma-Aldrich) prior to performing contractility experiments. Bronchial ring contractility measurements were performed in 15-ml organ baths as described above, with the following modifications: (a) a resting tension of 2 gf was applied; (b) rings were equilibrated for 2 hours; and (c) rings were first contracted with 120 mM KCl, and only rings that generated more than 4 mN tension were used for experiments. Rings were then washed and re-equilibrated and contractile responses were evaluated with increasing concentrations of MCh (Sigma-Aldrich) ranging from 10⁻⁹ to 10⁻³ M.

Measurements of ASM intracellular Ca²⁺ oscillations

The measurement protocol has been previously described (39). Briefly, murine lung slices were prepared from 6- to 12-week-old BALB/c mice. Mouse lungs were inflated with 1.0 ml of warm (37°C) 2% low-melting agarose through a catheter and 0.2 ml of air was injected to flush the agarose out of the airways. After agarose gelling in the whole lung by cooling to 4°C, a single lobe was removed and cut into serial sections of 100- μ m thickness with a vibratome (VT1000S LEICA) at 4°C. Slices were maintained in DMEM supplemented with antibiotics at 37°C and 7.5%

CO₂ overnight. Lung slices were labeled by Oregon Green 488 BAPTA-AM from Molecular Probes (Invitrogen; 20 μ M in HBSS containing 0.1% Pluronic F-127 from Molecular Probes and 100 μ M sulfobromophthalein) for 45 minutes at 30°C and de-esterified for 30 minutes at 30°C in HBSS containing 100 μ M sulfobromophthalein. Lung slices were placed in coverglass chambers (Labtek) immobilized with a slice anchor. Fluorescence imaging was performed with a NIKON spinning disk confocal microscope at 20 frames per second using a \times 10 Nikon objective. Changes in fluorescence intensity from selected regions of interest (5 \times 5 pixels) were analyzed using ImageJ software (NIH).

Fluorescence microscopy

To evaluate tissue-specific deletion of *Ptprj* in the airway smooth muscle of *Ptprj*^{TM- β /TM- β} ; *SMA-rTTA TetO-Cre* mice, lung tissue sections were stained for CD148 and α -SMA. The hamster mAb 8A1 (recognizing CD148) was used at a 1:200 dilution, followed by goat anti-hamster secondary antibody conjugated to Alexa488 (Molecular Probes; Invitrogen) at a 1:200 dilution. A directly conjugated anti- α -SMA Cy3 antibody (Sigma-Aldrich) was used at a 1:500 dilution.

Slides were visualized using a Zeiss Axiovert 200M microscope with a PCO Sencicam, and images were captured with Slidebook 5.0 software. Tracheal images were taken using a \times 40 oil objective. Bronchial airway images were taken using a \times 100 oil objective. To evaluate CD148 colocalization with α -SMA, a linear area transecting the smooth muscle strip was analyzed using ImageJ software (NIH).

Western blotting

Mouse tracheas were isolated and epithelial cells were removed by scraping the inner epithelial lining with a cotton swab. The posterior tracheal strip consisting primarily of smooth muscle was isolated under a dissecting microscope. Tracheal strips were stimulated for 5 minutes at 37°C with carbachol (10 μ M; Sigma-Aldrich) and then homogenized in ice-cold lysis buffer (150 mM NaCl; 50 mM Tris pH 8; 1% NP-40; 0.5% sodium deoxycholate; 0.1% SDS; and a cocktail of protease and phosphatase inhibitors). Lysates were centrifuged at 434,902 g for 30 minutes at 4°C and the supernatant was collected. Protein concentrations were determined using the BCA Protein Assay kit (Pierce Biotechnology). Samples were separated by a gradient gel (Life Technologies), transferred to a PVDF membrane (Millipore), and blocked for 30 minutes in Tris-buffered saline containing 5% nonfat milk. Membranes were incubated overnight with the indicated antibodies. After washing, membranes were incubated with a peroxidase-conjugated secondary antibody for 45 minutes, washed, and then developed with Plus-ECL reagent (PerkinElmer) or Super Signal West Femto Maximum Sensitivity Substrate (Thermo Scientific). Blots were developed using the Kodak Image Station 440CF and Kodak Molecular Imaging software (version 4.0.5).

Statistics

Two-way ANOVA was used for comparison of multiple groups using Prism (GraphPad Software), and when differences were statistically significant, this was followed with a Bonferroni *t* test for subsequent pairwise analysis. Differences with a *P* value of less than 0.05 were considered statistically significant. *P* values for comparisons of 2 different groups of mice were calculated with an unpaired 2-tailed Student's *t* test, and error bars were calculated as the SEM unless otherwise stated.

Study approval

All mice were housed in a specific pathogen-free animal facility at the University of California San Francisco (UCSF). Animals were treated according to protocols that were approved by the university animal care



ethics and veterinary committees in accordance with NIH guidelines. For human bronchial ring contractility experiments, cadaveric human lungs were obtained from brain-dead donors whose lungs could not be used for transplantation, and as with all cadaveric tissue, did not require approval by the UCSF Committee on Human Research.

Acknowledgments

We thank A. Roque for excellent assistance with animal husbandry. We also thank Weiss and Sheppard lab members, and members of the Sandler Asthma Basic Research Center (SABRE) for advice and helpful discussions. We acknowledge the Nikon Imaging Center at UCSF (<http://nic.ucsf.edu/>) for providing access to the spinning disk confocal microscope. This work is supported by the Rosalind Russell Medical Research Center for Arthritis Research, the Rheumatology Research Foundation's Physician Scientist Development Award and Investigator Award (to T.R. Katsumoto), the Rosalind Russell Medical Research Center Bechtel Award (to T.R. Katsu-

moto), a Cancer Research Institute Fellowship (to B.N. Manz), and an NIH grant (A1066120; to A. Weiss).

Received for publication August 17, 2012, and accepted in revised form February 7, 2013.

Address correspondence to: Arthur Weiss, University of California, San Francisco, 513 Parnassus Avenue, S-1032, San Francisco, California 94143-0795, USA. Phone: 415.476.1291; Fax: 415.502.5081; E-mail: aweiss@medicine.ucsf.edu.

Jing W. Zhu's present address is: Genentech Inc., South San Francisco, California, USA.

Makoto Kudo's present address is: Department of Internal Medicine and Clinical Immunology, Yokohama City University, Graduate School of Medicine, Yokohama, Japan.

1. Moorman JE, et al. National surveillance for asthma – United States, 1980–2004. *MMWR Surveill Summ.* 2007;56(8):1–54.
2. Guntur VP, Reimero CR. The potential use of tyrosine kinase inhibitors in severe asthma. *Curr Opin Allergy Clin Immunol.* 2011;12(1):68–75.
3. Wenzel SE, and WW. Severe asthma: lessons from the Severe Asthma Research Program. *J Allergy Clin Immunol.* 2007;119(1):14–21.
4. Seow CY, Schellenberg RR, Pare PD. Structural and functional changes in the airway smooth muscle of asthmatic subjects. *Am J Respir Crit Care Med.* 1998;158(5 pt 3):S179–S186.
5. Martin JG, Duguet A, Eidelman DH. The contribution of airway smooth muscle to airway narrowing and airway hyperresponsiveness in disease. *Eur Respir J.* 2000;16(2):349–354.
6. An SS, et al. Airway smooth muscle dynamics: a common pathway of airway obstruction in asthma. *Eur Respir J.* 2007;29(5):834–860.
7. Brightling CE, Bradding P, Symon FA, Holgate ST, Wardlaw AJ, Pavord ID. Mast-cell infiltration of airway smooth muscle in asthma. *N Engl J Med.* 2002;346(22):1699–1705.
8. James AL, et al. Airway smooth muscle thickness in asthma is related to severity but not duration of asthma. *Eur Respir J.* 2009;34(5):1040–1045.
9. Woodruff PG, et al. Hyperplasia of smooth muscle in mild to moderate asthma without changes in cell size or gene expression. *Am J Respir Crit Care Med.* 2004;169(9):1001–1006.
10. Wong WS. Inhibitors of the tyrosine kinase signaling cascade for asthma. *Curr Opin Pharmacol.* 2005;5(3):264–271.
11. Gaya A, et al. CD148, a new membrane tyrosine phosphatase involved in leukocyte function. *Leuk Lymphoma.* 1999;35(3–4):237–243.
12. Lin J, Zhu JW, Baker JE, Weiss A. Regulated expression of the receptor-like tyrosine phosphatase CD148 on hemopoietic cells. *J Immunol.* 2004;173(4):2324–2330.
13. Autschbach F, et al. Expression of the membrane protein tyrosine phosphatase CD148 in human tissues. *Tissue Antigens.* 1999;54(5):485–498.
14. Takahashi K, et al. Thrombospondin-1 acts as a ligand for CD148 tyrosine phosphatase. *Proc Natl Acad Sci U S A.* 2012;109(6):1985–1990.
15. Whiteford JR, Xian X, Chaussade C, Vanhaesebroeck B, Nourshargh S, Couchman JR. Syndecan-2 is a novel ligand for the protein tyrosine phosphatase receptor CD148. *Mol Biol Cell.* 2011;22(19):3609–3624.
16. Thomas SM, Brugge JS. Cellular functions regulated by Src family kinases. *Annu Rev Cell Dev Biol.* 1997;13:513–609.
17. Bjorge JD, Jakymiw A, Fujita DJ. Selected glimpses into the activation and function of Src kinase. *Oncogene.* 2000;19(49):5620–5635.
18. Sicheri F, Kuriyan J. Structures of Src-family tyrosine kinases. *Curr Opin Struct Biol.* 1997;7(6):777–785.
19. Zhu JW, Brdicka T, Katsumoto TR, Lin J, Weiss A. Structurally distinct phosphatases CD45 and CD148 both regulate B cell and macrophage immunoreceptor signaling. *Immunity.* 2008;28(2):183–196.
20. Pallen CJ. Protein tyrosine phosphatase alpha (PTPalpa): a Src family kinase activator and mediator of multiple biological effects. *Curr Top Med Chem.* 2003;3(7):821–835.
21. Su J, Muranjan M, Sap J. Receptor protein tyrosine phosphatase alpha activates Src-family kinases and controls integrin-mediated responses in fibroblasts. *Curr Biol.* 1999;9(10):505–511.
22. Roskoski Jr R. Src kinase regulation by phosphorylation and dephosphorylation. *Biochem Biophys Res Commun.* 2005;331(1):1–14.
23. Finkelman FD, Wills-Karp M. Usefulness and optimization of mouse models of allergic airway disease. *J Allergy Clin Immunol.* 2008;121(3):603–606.
24. Zhu JW, et al. Receptor-like tyrosine phosphatases CD45 and CD148 have distinct functions in chemoattractant-mediated neutrophil migration and response to *S. aureus*. *Immunity.* 2011;35(5):757–769.
25. Senis YA, et al. The tyrosine phosphatase CD148 is an essential positive regulator of platelet activation and thrombosis. *Blood.* 2009;113(20):4942–4954.
26. Kuperman DA, et al. Direct effects of interleukin-13 on epithelial cells cause airway hyperreactivity and mucus overproduction in asthma. *Nat Med.* 2002;8(8):885–889.
27. Woodruff PG, et al. T-helper type 2-driven inflammation defines major subphenotypes of asthma. *Am J Respir Crit Care Med.* 2009;180(5):388–395.
28. Wills-Karp M. Immunologic basis of antigen-induced airway hyperresponsiveness. *Annu Rev Immunol.* 1999;17:255–281.
29. Lloyd CM, Hessel EM. Functions of T cells in asthma: more than just T(H)2 cells. *Nat Rev Immunol.* 2010;12(12):838–848.
30. Kim HY, DeKruyff RH, Umetsu DT. The many paths to asthma: phenotype shaped by innate and adaptive immunity. *Nat Immunol.* 2010;11(7):577–584.
31. Yu M, et al. Identification of an IFN-gamma/mast cell axis in a mouse model of chronic asthma. *J Clin Invest.* 2011;121(8):3133–3143.
32. Alcorn JF, Crowe CR, Kolls JK. TH17 cells in asthma and COPD. *Annu Rev Physiol.* 2010;72:495–516.
33. Stevenson CS, Birrell MA. Moving towards a new generation of animal models for asthma and COPD with improved clinical relevance. *Pharmacol Ther.* 2011;130(2):93–105.
34. Wills-Karp M, et al. Interleukin-13: central mediator of allergic asthma. *Science.* 1998;282(5397):2258–2261.
35. Perl AK, Wert SE, Nagy A, Lobe CG, Whitsett JA. Early restriction of peripheral and proximal cell lineages during formation of the lung. *Proc Natl Acad Sci U S A.* 2002;99(16):10482–10487.
36. Chen C, et al. Integrin alpha9beta1 in airway smooth muscle suppresses exaggerated airway narrowing. *J Clin Invest.* 2012;122(8):2916–2927.
37. Billington CK, Penn RB. Signaling and regulation of G protein-coupled receptors in airway smooth muscle. *Respir Res.* 2003;4:2.
38. Somlyo AP, Somlyo AV. Signal transduction by G-proteins, rho-kinase and protein phosphatase to smooth muscle and non-muscle myosin II. *J Physiol.* 2000;522(pt 2):177–185.
39. Perez JF, Sanderson MJ. The contraction of smooth muscle cells of intrapulmonary arterioles is determined by the frequency of Ca²⁺ oscillations induced by 5-HT and KCl. *J Gen Physiol.* 2005;125(6):555–567.
40. Blake RA, et al. SU6656, a selective src family kinase inhibitor, used to probe growth factor signaling. *Mol Cell Biol.* 2000;20(23):9018–9027.
41. Pertel T, Zhu D, Panettieri RA, Yamaguchi N, Emala CW, Hirshman CA. Expression and muscarinic receptor coupling of Lyn kinase in cultured human airway smooth muscle cells. *Am J Physiol Lung Cell Mol Physiol.* 2006;290(3):L492–L500.
42. Shore SA. Airway smooth muscle in asthma – not just more of the same. *N Engl J Med.* 2004;351(6):531–532.
43. Deshpande DA, et al. Bitter taste receptors on airway smooth muscle bronchodilate by localized calcium signaling and reverse obstruction. *Nat Med.* 2010;16(11):1299–1304.
44. Deshpande DA, Penn RB. Targeting G protein-coupled receptor signaling in asthma. *Cell Signal.* 2006;18(12):2105–2120.
45. Zikherman J, et al. CD45-Csk phosphatase-kinase titration uncouples basal and inducible T cell receptor signaling during thymic development. *Immunity.* 2010;32(3):342–354.
46. Barnes PJ, Chung KF, Page CP. Inflammatory mediators of asthma: an update. *Pharmacol Rev.* 1998;50(4):515–596.
47. Brown MT, Cooper JA. Regulation, substrates and functions of src. *Biochim Biophys Acta.* 1996;1287(2–3):121–149.
48. Luttrell DK, Luttrell LM. Not so strange bedfellows: G-protein-coupled receptors and Src family kinases. *Oncogene.* 2004;23(48):7969–7978.
49. McGarrigle D, Huang XY. GPCRs signaling directly through Src-family kinases. *Sci STKE.* 2007;



- 2007(392):pe35.
50. Tolloczko B, Turkewitsch P, Choudry S, Bisotto S, Fixman ED, Martin JG. Src modulates serotonin-induced calcium signaling by regulating phosphatidylinositol 4,5-bisphosphate. *Am J Physiol Lung Cell Mol Physiol*. 2002;282(6):L1305-L1313.
51. Xu Y, Harder KW, Huntington ND, Hibbs ML, Tarlinton DM. Lyn tyrosine kinase: accentuating the positive and the negative. *Immunity*. 2005;22(1):9-18.
52. Beavitt SJ, et al. Lyn-deficient mice develop severe, persistent asthma: Lyn is a critical negative regulator of Th2 immunity. *J Immunol*. 2005;175(3):1867-1875.
53. Parameswaran K, Radford K, Zuo J, Janssen LJ, O'Byrne PM, Cox PG. Extracellular matrix regulates human airway smooth muscle cell migration. *Eur Respir J*. 2004;24(4):545-551.
54. Parameswaran K, et al. Modulation of human airway smooth muscle migration by lipid mediators and Th-2 cytokines. *Am J Respir Cell Mol Biol*. 2007;37(2):240-247.
55. Krymskaya VP, et al. Src is necessary and sufficient for human airway smooth muscle cell proliferation and migration. *FASEB J*. 2005;19(3):428-430.
56. Sakai H, et al. Involvement of Src family kinase activation in angiotensin II-induced hyperresponsiveness of rat bronchial smooth muscle. *Peptides*. 2010;31(12):2216-2221.
57. Knock GA, et al. Interaction between src family kinases and rho-kinase in agonist-induced Ca²⁺-sensitization of rat pulmonary artery. *Cardiovasc Res*. 2008;77(3):570-579.
58. Sanderson MJ, Delmotte P, Bai Y, Perez-Zoghbi JF. Regulation of airway smooth muscle cell contractility by Ca²⁺ signaling and sensitivity. *Proc Am Thorac Soc*. 2008;5(1):23-31.
59. Jayaraman T, Ondrias K, Ondriasova E, Marks AR. Regulation of the inositol 1,4,5-trisphosphate receptor by tyrosine phosphorylation. *Science*. 1996;272(5267):1492-1494.
60. Kawasaki BT, Liao Y, Birnbaumer L. Role of Src in C3 transient receptor potential channel function and evidence for a heterogeneous makeup of receptor- and store-operated Ca²⁺ entry channels. *Proc Natl Acad Sci U S A*. 2006;103(2):335-340.
61. Vazquez G, Wedel BJ, Kawasaki BT, Bird GS, Putney JW Jr. Obligatory role of Src kinase in the signaling mechanism for TRPC3 cation channels. *J Biol Chem*. 2004;279(39):40521-40528.
62. Hisatsune C, et al. Regulation of TRPC6 channel activity by tyrosine phosphorylation. *J Biol Chem*. 2004;279(18):18887-18894.
63. Balavenkatraman KK, et al. DEP-1 protein tyrosine phosphatase inhibits proliferation and migration of colon carcinoma cells and is upregulated by protective nutrients. *Oncogene*. 2006;25(47):6319-6324.
64. Jandt E, Denner K, Kovalenko M, Ostman A, Bohmer FD. The protein-tyrosine phosphatase DEP-1 modulates growth factor-stimulated cell migration and cell-matrix adhesion. *Oncogene*. 2003;22(27):4175-4185.
65. Chabot C, Spring K, Gratton JP, Elchebly M, Royal I. New role for the protein tyrosine phosphatase DEP-1 in Akt activation and endothelial cell survival. *Mol Cell Biol*. 2009;29(1):241-253.
66. Pera IL, et al. The rat tyrosine phosphatase eta increases cell adhesion by activating c-Src through dephosphorylation of its inhibitory phosphotyrosine residue. *Oncogene*. 2005;24(19):3187-3195.
67. Zhang W, Gunst SJ. Interactions of airway smooth muscle cells with their tissue matrix: implications for contraction. *Proc Am Thorac Soc*. 2008;5(1):32-39.
68. Wang XJ, et al. Thrombospondin-1-induced migration is functionally dependent upon focal adhesion kinase. *Vasc Endovascular Surg*. 2008;42(3):256-262.
69. de Boer J, et al. Transgenic mice with hematopoietic and lymphoid specific expression of Cre. *Eur J Immunol*. 2003;33(2):314-325.
70. Kudo M, et al. IL-17A produced by alphabeta T cells drives airway hyper-responsiveness in mice and enhances mouse and human airway smooth muscle contraction. *Nat Med*. 2012;18(4):547-554.